Carbohydrate Polymers 94 (2013) 940–945

Contents lists available at SciVerse ScienceDirect

Carbohydrate Polymers

journal homepage: www.elsevier.com/locate/carbpol

Scalable ionic gelation synthesis of chitosan nanoparticles for drug delivery in static mixers

Yuancai Dong[a,*], Wai Kiong Ng[a], Shoucang Shen[a], Sanggu Kim[a], Reginald B.H. Tan[a,b,**]

[a] Institute of Chemical and Engineering Sciences, 1 Pesek Road, Jurong Island, Singapore 627833, Singapore
[b] Department of Chemical and Biomolecular Engineering, National University of Singapore, 4 Engineering Drive 4, Singapore 119260, Singapore

ARTICLE INFO

Article history:
Received 9 November 2012
Received in revised form 8 February 2013
Accepted 9 February 2013
Available online 18 February 2013

Keywords:
Chitosan
Nanoparticles
Ionic gelation
Static mixer
Drug delivery

ABSTRACT

The purpose of this study is to synthesize chitosan (CS) nanoparticles (NPs) by ionic gelation with tripolyphosphate (TPP) as crossslinker in static mixers. The proposed static mixing technique showed good control over the ionic gelation process and 152–376 nm CS NPs were achieved in a continuous and scalable mode. Increasing the flow rates of CS:TPP solution streams, decreasing the CS concentration or reducing the CS:TPP solution volume ratio led to the smaller particles. Sylicylic acid (SA) was used as a model drug and successfully loaded into the CS NPs during the fabrication process. Our work demonstrates that ionic gelation–static mixing is a robust platform for continuous and large scale production of CS NPs for drug delivery.

1. Introduction

Chitosan (CS) is a linear copolymer of randomly distributed ß-(1,4)-linked D-glucosamine and N-acetyl-D-glucosamine. Owing to its unique structure, CS possesses numerous attractive features, such as good biocompatibility, biodegradability, permeation enhancing effect, cationic properties, etc. These advantages render CS widely applied in the pharmaceutical and tissue engineering fields. Especially, nanoparticles (NPs) made of CS have been undergoing extensive exploitation for delivery of drugs, proteins/peptides, genes, DNA, etc. (Katas & Alpar, 2006; Krauland & Alonso, 2007; Li, Wang, Peng, She, & Kong, 2011; Makhlof, Tozuka, & Takeuchi, 2011; Saboktakin, Tabatabaee, Maharramov, & Ramazanov, 2010; Xu & Du, 2003; Zhang, Oh, Allen, & Kumacheva, 2004). CS NPs can be synthesized via a number of techniques. These include electrospray, microemulsion, ionic gelation, emulsification solvent diffusion, etc. (Agnihotri, Mallikarjuna, & Aminabhavi, 2004; Hamidi, Azadi, & Rafiei, 2008; Liu, Jiao, Wang, Zhou, & Zhang, 2008; Nagpal, Singh, & Mishra, 2010; Songsurang, Praphairaksit, Siraleatmukul, & Muangsin, 2011; Zhang & Kawakami, 2010). Among them, ionic gelation with tripolyphosphate (TPP) as the crosslinker is the mostly adopted technique to fabricate CS NPs, since this method is simple, mild, less toxic and suitable for scaling up. In addition, the size of the achieved NPs can be precisely tuned by adjusting the process parameters, e.g. CS and TPP concentration, CS/TPP weight ratio and volume ratio, pH value, etc. For this method, CS is dissolved in the acidic solution, to which aqueous TPP solution is added. Inter- and intracrosslinking (gelation) of the protonated amine group on the CS molecules with the negatively charged TPP anions occurs spontaneously leading to the formation of the CS particles. By selecting the appropriate conditions, the formed particles can be controlled in the submicron range. Loading a drug into CS NPs can be achieved by addition of the drug to the CS (or TPP) solution prior to the ionic gelation process or adsorption of the drug onto the preformed blank CS NPs. The CS/TPP particles-formation can be divided into the two processes: (1) mixing of the CS and TPP aqueous solution and dispersion of the TPP anions within the CS molecules and (2) crosslinking (i.e. gelation) between the protonated amine groups and TPP anions. These two processes occur in sequence initially but likely to proceed in parallel subsequently, since the CS/TPP complexation is almost instantaneous and will start while mixing is probably still occurring. Therefore, rapid mixing favors the fast and uniform dispersion of the TPP anions within the chitosan chains leading to the formation of the smaller NPs with narrower polydispersity; while slow mixing causes inhomogeneous dispersion of TPP anions resulting in larger particles with wider size distribution. In the literature, only a few studies have described the significance of mixing on the

* Corresponding author. Tel.: +65 67963864; fax: +65 63166183.
** Corresponding author at: Department of Chemical and Biomolecular Engineering, National University of Singapore, 4 Engineering Drive 4, Singapore 119260, Singapore. Tel.: +65 67963855; fax: +65 63166183.
E-mail addresses: dong_yuancai@ices.a-star.edu.sg (Y. Dong), reginald_tan@ices.a-star.edu.sg (R.B.H. Tan).

0144-8617/$ – see front matter © 2013 Elsevier Ltd. All rights reserved.
http://dx.doi.org/10.1016/j.carbpol.2013.02.013

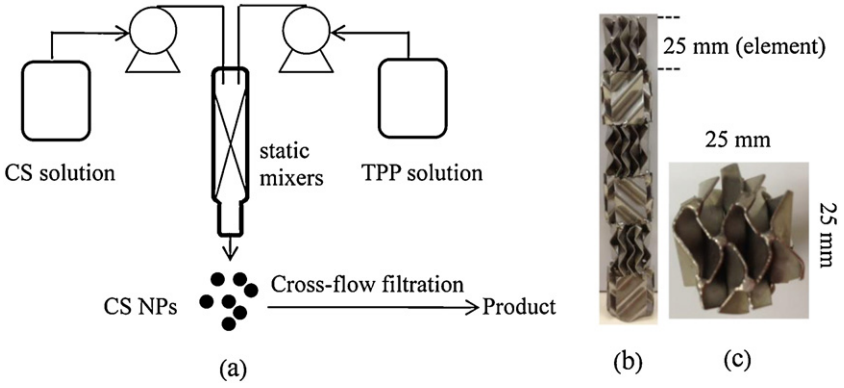

Fig. 1. Scheme of ionic gelation synthesis of CS NPs in static mixers (a), image of 1-segment static mixers composed of 6 elements (b) and top view of static mixers (c).

formation of CS NPs (Nasti et al., 2009; Fan, Yan, Xu, & Ni, 2012). This is probably due to the fact that, most of the reported studies synthesized CS NPs on lab scale. In such a small batch system (e.g. volume from several to tens of milliliter), rapid and uniform mixing can always be achieved by magnetic stirring ensuring the formation of the small NPs. For a large scale production process, however, mixing becomes prominent, as the stirred tank used in the industry is generally characteristic of a slow and inhomogeneous mixing and therefore not a good choice (Dong, Ng, Hu, Shen, & Tan, 2010). Some mixing-intensification equipments are needed for a large scale ionic gelation production of CS NPs. For example, Loh et al. used spinning disc as a process intensification apparatus for mass-production of CS NPs by ionic gelation (Loh, Schneider, Carter, Saunders & Lim, 2010).

Static mixers are one of widely used process-intensification equipments in industry. They are composed of a number of tortuous elements with same configuration. As the flows to be mixed move through the mixers, the tortuous motionless elements continuously convolute and recombine the streams to complete mixing rapidly. A number of additional advantages can also be conferred by static mixers, such as low energy requirement, compact space requirement, low cost, continuous operation, etc. (Thakur, Vial, Nigam, Nauman, & Djelveh, 2003). Our group has used static mixers as process intensification equipment for large scale synthesis of drug nanoparticles and solid lipid nanoparticles (Dong et al., 2010; Dong, Ng, Shen, Kim, & Tan, 2012; Hu, Ng, Dong, Shen, & Tan, 2011). In this work, we aimed to develop a scalable ionic gelation process using static mixers to produce CS NPs in a continuous mode. To our knowledge, synthesis of CS NPs with static mixers has not been reported in literature. Effects of the process parameters, such as number of mixing elements, flow rate, CS concentration and CS/TPP volume ratio on the size of the blank CS NPs (without drug) were explored. Sylicylic acid (SA) was used a model compound and loaded into the CS NPs during the synthesis process for potential intravenous administration. Effect of the drug input on the size and loading efficiency was examined. Morphology of the CS NPs was imaged by field emission scanning electron microscopy (FESEM). Finally, the SA release pattern from CS NPs was assessed in Phosphate Buffer Solution (PBS, pH 7.4).

2. Materials and methods

2.1. Materials

Chitosan hydrochloride (CS) with Mw 200,000–500,000 and deacetylation degree 91.8% was purchased from Xianju Tengwang Chitosan Factory, China. TPP (purity ≥ 98.0%) was supplied by Sigma–Aldrich. The model drug sylicylic acid (SA, purity ≥ 99.0%) was obtained from Sigma. Deionized (D.I.) water was used throughout the study.

2.2. Synthesis of CS NPs in static mixers

Blank and SA-loaded CS NPs were synthesized by ionic gelation in static mixers. SMV DN25 static mixers with a scale of 25 mm were provided by Sulzer Chemtech (Switzerland). Six elements were welded together by being offset at 90° to be one segment (Fig. 1b and c). 1–3 segments were inserted into the glass tube in operation. The detailed scheme of synthesis of CS NPs by ionic gelation in static mixers was illustrated in Fig. 1a. The weight ratio of CS to TPP was kept to be 5:1 throughout the work, as the preliminary results showed that the CS NPs achieved at this ratio were comparatively small and uniform (data not shown). In brief, CS and TPP were dissolved in D.I. water, which were pumped into static mixers by peristaltic pumps. CS NPs were formed spontaneously upon mixing inside static mixers. 300 ml suspension was continuously collected at the exit of static mixers for size and zeta potential measurements. Drug-loaded CS NPs were fabricated in the same way as the blank ones except that 10 or 20 wt% SA (to the weight of CS) was co-dissolved in the CS solution. To remove unloaded drug, the achieved 300 ml suspension was purified with cross-flow filtration (Vivaflow 50, Mw cutoff 100,000) and condensed to 50 ml, which was refilled by D.I. water to 300 ml for repeated cross-flow filtration. Such purification process was performed thrice and 50 ml drug-loaded suspension was achieved finally. A portion of purified SA-loaded CS NPs suspension was directly lyophilized to obtain the powders for drug loading analysis; while a portion of purified SA-loaded CS NPs was lyophilized with 4 times weight sucrose as lyoprotectant to achieve powders for dissolution studies. Some basic process parameters were: (1) the number of mixing elements was 12, (2) the flow rate of CS and TPP solution were 250 and 50 ml/min, respectively, (3) the CS concentration was 0.5 mg/ml and (4) the volume ratio of CS to TPP (CS:TPP) was 5:1. When the effect of one process parameter was examined, the other parameters were kept unchanged unless otherwise described.

2.3. Size and zeta potential (ZP) measurement

Dynamic laser light scattering technique (Nano-Zetasizer, Malvern) was used to measure the size of the CS NPs. This technique first determines the diffusivity of the particles in the suspension based on the time-dependent fluctuations in the intensity of scattered light resulting from the Brownian motion. Size of the particles is thus calculated from the Stokes–Einstein equation. Before measurement, the particles concentration was diluted to ca. 0.25 mg/ml and the measurement was performed at 25 °C. Z-average size and the polydispersity index (PDI) was reported (mean ± SD, $n = 3$). ZP of

the SA-loaded CS NPs was also determined by Nanozeta Sizer using electrophoretic light scattering technique. The measurement was performed in D.I. water at 25 °C. The mean and SD of the triplicate measurements was reported.

2.4. Drug loading efficiency

Drug loading was measured based on the method adopted from the references (Anal, Stevens, & Lopez, 2006; Ji, Hao, Wu, Huang, & Xu, 2011). Briefly, 4 mg freeze-dried SA-loaded CS NPs was dissolved into 8 ml 0.1 M HCl overnight. The solution was then centrifuged at 11,000 rpm for half an hour and 1 ml supernatant was collected for the HPLC analysis (Agilent 1100). The column was Eclipse XDB C_{18} (4.6 mm × 250 mm, 5 μm). The mobile phase was a mixture of 40% water, 59% methanol and 1% acetic acid and delivered at 1 ml/min. SA was analyzed at 297 nm. Drug loading and loading efficiency was calculated by the following equations:

$$\text{Drug loading}\,\% = \frac{\text{drug amount in 4 mg powder}}{\text{4 mg powder}} \times 100\%$$

$$\text{Loading efficiency}\,\% = \frac{\text{total drug loaded in NPs}}{\text{total drug input}} \times 100\%$$

2.5. Morphology

Morphology of the CS NPs was observed by the field emission scanning electron microscope (FESEM, JEOL JSM-6700F). A drop of CS NPs suspension was deposited onto the copper tape and air dried, which was then sputtered by gold for 120 s. The visualization was then performed at a voltage of 5 kv and a current of 10 A.

2.6. X-ray diffraction (XRD)

Crystallinity of the CS, SA, blank CS NPs and drug-loaded CS NPs were assessed by D8-ADVANCE (BRUKER) X-ray diffractometer from 5 to 40° (2θ) at a step of 0.017° using Cu Kα radiation.

2.7. In vitro drug release

The in vitro release patterns of SA from CS NPs were evaluated by dialysis bag method over 24 h. Briefly, a certain amount of lyophilized SA-loaded CS NPs (containing 230 μg drug) was suspended in 5 ml Phosphate Buffer Solution (PBS, pH 7.4) in a sealed dialysis bag (Spectra/Por 7, 50,000 MW cut-off), which was incubated in 50 ml PBS-containing bottle. The release was performed in a water-bath shaker with a speed of 50 rpm at 37 °C. At specific time, 0.5 ml release medium was collected for HPLC analysis and 0.5 ml fresh PBS was refilled to continue the release studies.

2.8. Statistical analysis

Statistical analysis was conducted with the Package for Encyclopedia Medical Statistics (PEMS). p values less than 0.05 were considered to be statistically significant. All statistical tests were two-tailed

3. Results and discussion

3.1. Effect of number of mixing elements

Continuous ionic gelation synthesis of CS NPs was performed in static mixers. Effect of the number of mixing elements on the size was first explored. Previous studies have shown that there exists a minimum number of mixing elements to ensure the complete mixing inside static mixers (Bourne, Lenzner, & Petrozzi, 1992). It can be seen from Table 1 that, the size of CS NPs prepared in static mixers with 6 and 12 elements was 228 ± 2 and 232 ± 5 nm, respectively, which are not of significant difference ($p > 0.05$). Increasing the number of mixing elements to 18 led to a minor size decrease to 217 ± 1 nm. It is also found that CS NPs prepared in static mixers with 12 and 18 elements exhibited a slight decrease in PDI in comparison with those prepared in 6-element static mixers. The results demonstrate that static mixers with 6 elements are sufficient to control the mixing and gelation process to achieve the CS particles in the submicron range. Taking into account the size, PDI and ease of operation, static mixers with 12 elements was used in the subsequent experiments.

Table 1
Effect of process parameters on the size and PDI of CS NPs (mean ± SD, $n = 3$).

Samples		Size (nm)	PDI
Process parameters	Variables		
Number of mixing elements	6	228 ± 2	0.245 ± 0.004
	12	232 ± 5	0.201 ± 0.025
	18	217 ± 1	0.210 ± 0.020
Flow rate (ml/min, CS:TPP)	125:25	255 ± 8	0.251 ± 0.012
	250:50	232 ± 5	0.201 ± 0.025
	375:75	224 ± 2	0.238 ± 0.020
	500:100	239 ± 5	0.246 ± 0.026
Chitosan concentration (mg/ml)	0.25	152 ± 1	0.149 ± 0.012
	0.50	232 ± 5	0.201 ± 0.025
	0.75	307 ± 4	0.334 ± 0.015
	1.0	377 ± 6	0.459 ± 0.056
Volume ratio (CS:TPP)	7:1	267 ± 3	0.249 ± 0.018
	5:1	232 ± 5	0.201 ± 0.025
	3:1	218 ± 1	0.182 ± 0.026

3.2. Effect of CS:TPP flow rate

Keeping the CS:TPP weight ratio and volume ratio both to be 5:1, effect of the flow rate on the size of the CS NPs was investigated. As listed in Table 1, CS NPs prepared at the flow rate of 125:25 (ml/min, CS:TPP) had a size of 255 ± 8 nm, which was reduced to 232 ± 5 and 224 ± 2 nm with increasing the flow rate to 250:50 and 375:75, respectively. This indicates that increasing the flow rate enhances the mixing efficiency (Bourne & Maire, 1991; Thakur et al., 2003), which facilitates the rapid dispersion of TPP anions within CS molecules resulting in the smaller particles. Further increasing the flow rate to 500:100, however, produced relatively larger particles, i.e. 239 ± 5 nm. This is probably due to the fact that, at high flow rate, the CS and TPP solution flow streams, being impinged on the mixing elements at high velocity, splash outwards causing the impairment of mixing efficiency and the slightly larger particles are thus formed.

3.3. Effect of CS concentration

Increasing the CS concentration from 0.25 to 0.5, 0.75 and 1.0 mg/ml caused radical size increase from 152 ± 1 to 232 ± 5, 307 ± 4 and 377 ± 6 nm, respectively ($p < 0.05$), as shown in Table 1. In addition, the PDI was dramatically increased from 0.149 ± 0.012 to 0.459 ± 0.056 correspondingly ($p < 0.05$). These results reveal that higher CS concentration produces larger NPs with wider size distribution. This phenomenon can be explained by the ease of dispersion of TPP anions within CS molecules at different concentrations. In low CS concentration solution, the CS molecule chains exist in extended conformation due to the repulsion between the positively charged amine groups. Accordingly, there exists

Table 2
Effect of drug input on the size, PDI, ZP, loading efficiency and drug loading (mean ± SD, $n = 3$).

Drug input (%)	Size (nm)	PDI	ZP (mv)	Drug loading (%)	Loading efficiency (%)
0	232 ± 5	0.201 ± 0.025	38.3 ± 2.0	–	–
10	208 ± 4	0.239 ± 0.005	42.9 ± 1.6	2.27 ± 0.19	29.50 ± 2.51
20	177 ± 2	0.276 ± 0.011	42.9 ± 1.7	4.71 ± 0.05	33.00 ± 0.37

large space within CS molecules allowing the rapid dispersion of TPP anions. The subsequent uniform inter- and intra-crosslinking between the protonated amine group and TPP anions is therefore ensured for producing smaller and more uniform NPs. With the CS concentration increase, the CS molecules come closer and start to entangle or aggregate. Dispersion of TPP anions within CS molecules is thus relatively difficult and inhomogeneous resulting in the larger particles (Berger et al., 2004; Fan et al., 2012; Gao & Wan, 2006).

3.4. Effect of CS:TPP volume ratio

Keeping the flow rate of CS solution (0.5 mg/ml) and the CS:TPP weight ratio to be 250 ml/min and 5:1, effect of the CS:TPP volume ratio on the size was explored. As displayed in Table 1, reducing the CS:TPP volume ratio from 7:1 to 5:1 and 3:1 resulted in the size decrease from 267 ± 3 to 232 ± 5 and 218 ± 1 nm ($p < 0.05$), respectively. Since the CS:TPP volume ratio was adjusted in this work by keeping the CS solution flow rate constant (i.e. 250 ml/min) while varying the TPP flow rate to 35.7, 50 and 83.3 ml/min for the CS:TPP volume ratio 7:1, 5:1 and 3:1, the observed size decrease accordingly could be ascribed to the fact that, with increasing the flow rate of TPP solution (i.e. reducing the CS:TPP volume ratio), a larger volume of the water involved in the gelation process renders the CS/TPP system more diluted, which speeds up the dispersion of TPP anions within CS molecules leading to the formation of the smaller NPs (Fan et al., 2012).

The above results demonstrate that static mixing is able to control over the ionic gelation process and produce the CS NPs in a continuous and scalable mode. Size of CS NPs is influenced by the process parameters, such as number of mixing elements, flow rate, CS concentration, etc. Since the pK_a of CS is approximately 6.5 while TPP exhibits five pK_a from 1.0 to 8.5 (Lim & Seib, 1993), pH also plays a crucial role in determining the properties of the achieved CS NPs, such as size, stability, swelling, drug loading, release, etc. It is reported that pH 4–6 is beneficial to maintain the stability of the CS NPs (Nasti et al., 2009). In this work, the pH of CS solution from 0.25 to 1 mg/ml was approximately 3.8–3.6; while the pH of TPP solution (0.25–1 mg/ml) was 8.9–9.1. The obtained CS NPs suspension from 0.25 and 1 mg/ml CS solution had a pH of 5.1 and 5.7. All other CS NPs samples had a pH of 5.4. It can be seen that the pH of the synthesized CS NPs in this work is favorable for maintaining the stability of the CS NPs. Effect of the pH is thus not further examined.

3.5. SA-loaded CS NPs

SA is a small molecule with certain water solubility (~2 mg/ml) and thus suitable for application in aqueous ionic gelation synthesis and the subsequent cross-flow filtration purification process. It is therefore used as a model compound in this work to test the suitability of the static mixing-ionic gelation technique for making drug-loaded CS NPs. Effect of the drug input on the size, PDI, ZP, drug loading and loading efficiency is listed in Table 2. In comparison with the blank (without drug) NPs, the size of the CS NPs prepared from 10 wt% and 20 wt% drug input was drastically decreased from 232 ± 5 to 208 ± 4 and 177 ± 2 nm, respectively ($p < 0.05$). This result is contrary to most of other drug-loaded NP systems, such as polymeric NPs, in which, loading a drug would not cause an obvious change in size. This phenomenon might be explained by the screening effect of the SA. In aqueous solution without SA, the CS molecules take the relatively extended and stiff conformation due to the repulsion between the positively charged amine groups. When SA is present, the positive charge is screened leading to a reduced repulsion. The CS molecules are thus more contracted and flexible resulting in the formation of the smaller NPs (Fan et al., 2012; Jonassen, Kjøniksen, & Hiorth, 2012). The ZP of both blank and SA-loaded CS NPs was around +40 mv, which is attributed to the positively charged amine groups non-neutralized by TPP anions. For 10 wt% and 20 wt% drug input, the final drug loading was 2.27 ± 0.19 and 4.71 ± 0.05%, which corresponded to the loading efficiency of 29.50 ± 2.51 and 33.00 ± 0.37%, respectively. The low loading efficiency could be ascribed to the fact that SA is a small molecule with certain water solubility. Unlike water-soluble large molecules like proteins, SA lacks strong interaction (e.g. physical entanglement) with CS NPs, which makes it easier to escape from encapsulation.

3.6. Morphology

Morphology of the typical CS NPs is shown in Fig. 2. The CS NPs exhibited a nearly spherical shape and the size was around 200 nm, which is consistent with the results obtained by the DLS.

3.7. XRD

Fig. 3 illustrates the XRD patterns of SA, CS, blank CS NPs and drug-loaded CS NPs. SA exhibited intense peaks at 2θ of 11°, 17.2° and 25.3° (Fig. 3b). CS showed one sharp peak at 2θ of 32° and two weak peak at 2θ of 11.7° and 18.7° (Fig. 3a). For the blank and drug-loaded CS NPs (Fig. 3c–e), the intensity of two peaks at 2θ of 11.7° and 18.7° was decreased in comparison with the CS while the intense peak at 2θ of 32° disappeared indicating the increased amorphous state of the NPs matrix.

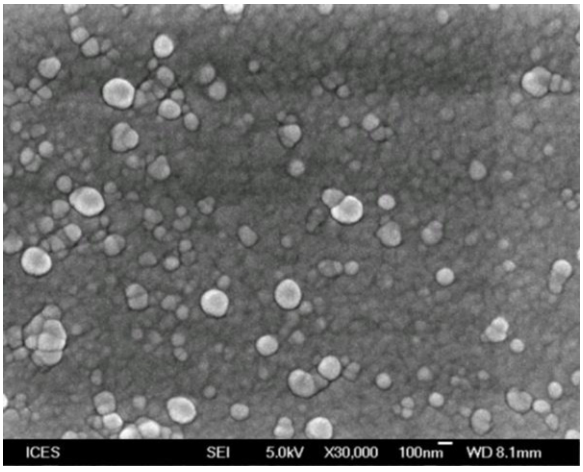

Fig. 2. SEM image of typical CS NPs.

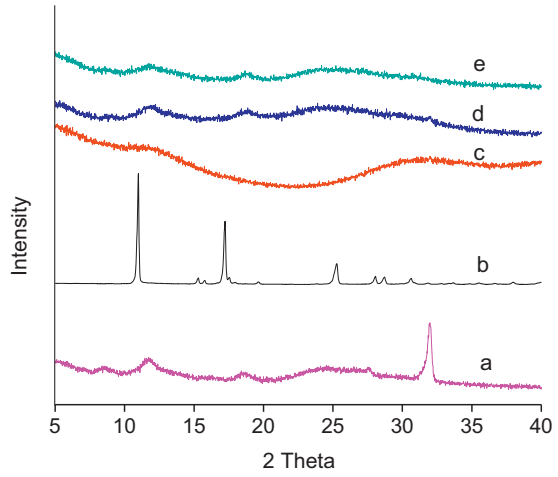

Fig. 3. XRD patterns of CS (a), SA (b), blank CS NPs (c) and drug-loaded NPs with 10 wt% (d) and 20 wt% (e) drug input.

3.8. In vitro release

Fig. 4 shows the release patterns of SA from CS NPs with the drug loading of 2.27% (curve a) and 4.71% over 24 h (curve b). It can be observed that these two CS NPs with different drug loading had the same release rate under the experimental conditions and there's no significant difference for the cumulative SA released at any analysis time ($p > 0.05$). Drug-loaded CS NPs exhibited a triphasic release profile with an initial burst followed by slower and constant release rates. Within 0.5 h, 35% of the loaded drug was released out from both NPs, which was increased to 53% in 1 h. This initial burst was mostly ascribed to those drugs located on or near the particles surface, which rapidly diffused out upon contact with the release medium. The release rate was then relatively slow: only 18% drug was released between 1 and 2 h and it was further reduced to 8% between 2 and 3 h. 79% of the loaded drug was released within 3 h. After that, CS NPs showed a much slower rate with only 11% released between 3 and 8 h. The slow release rate could be due to the drug located inside the NPs, which needs a longer diffusion path from the interior to the release medium. Totally, 90% drug was released within 8 h. Overall, SA exhibited a rapid release from CS NPs, which could be ascribed to the amorphous state of the NPs matrix and the increased swelling of CS NPs due to the decreased crosslinking density in pH 7.4 medium.

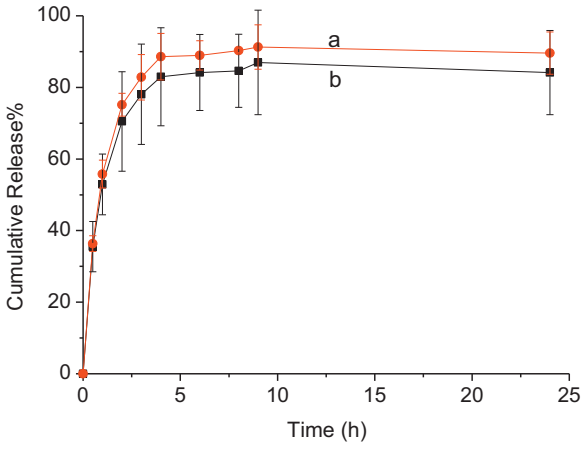

Fig. 4. In vitro release of SA-loaded CS NPs.

4. Conclusions

CS NPs with 152–376 nm were continuously produced by the ionic gelation-static mixing platform in a scalable mode. Size of the CS NP can be adjusted by some process parameters, such as CS concentration, flow rate, CS:TPP volume ratio, etc.; while the productivity can be controlled by the CS concentration and flow rate. Loading a model drug SA was successfully performed by the developed technique. This work demonstrates the robustness of ionic gelation-static mixing for continuous and potential large scale synthesis of CS NPs.

Acknowledgement

This work was supported by project grant ICES/07-122B01 from Agency for Science, Technology and Research (A*STAR), Singapore.

References

Agnihotri, S. A., Mallikarjuna, N. N., & Aminabhavi, T. M. (2004). Recent advances on chitosan-based micro- and nanoparticles in drug delivery. *Journal of Controlled Release*, *100*, 5–28.

Anal, A. K., Stevens, W. F., & Lopez, C. R. (2006). Ionotropic cross-linked chitosan microspheres for controlled release of ampicillin. *International Journal of Pharmaceutics*, *312*, 166–173.

Berger, J., Reist, M., Mayer, J. M., Felt, O., Peppas, N. A., & Gurny, R. (2004). Structure and interactions in covalently and ionically crosslinked chitosan hydrogels for biomedical applications. *European Journal of Pharmaceutics and Biopharmaceutics*, *57*, 19–34.

Bourne, J. R., & Maire, H. (1991). Micromixing and fast chemical reactions in static mixers. *Chemical Engineering and Processing*, *30*, 23–30.

Bourne, J. R., Lenzner, J., & Petrozzi, S. (1992). Micromixing in static mixers: An experimental study. *Industrial and Engineering Chemistry Research*, *31*, 1216–1222.

Dong, Y., Ng, W. K., Hu, J., Shen, S. C., & Tan, R. B. H. (2010). A continuous and highly effective static mixing process for antisolvent precipitation of nanoparticles of poorly water-soluble drugs. *International Journal of Pharmaceutics*, *386*, 256–261.

Dong, Y., Ng, W. K., Shen, S., Kim, S., & Tan, R. B. H. (2012). Solid lipid nanoparticles: Continuous and potential large-scale nanoprecipitation production in static mixers. *Colloids and Surfaces B: Biointerface*, *94*, 68–72.

Fan, W., Yan, W., Xu, Z., & Ni, H. (2012). Formation mechanism of monodisperse, low molecular weight chitosan nanoparticles by ionic gelation technique. *Colloids and Surface B: Biointerface*, *90*, 21–27.

Gao, Q., & Wan, A. (2006). Effects of molecular weight, degree of acetylation and ionic strength on surface tension of chitosan in dilute solution. *Carbohydrate Polymers*, *64*, 29–36.

Hamidi, M., Azadi, A., & Rafiei, P. (2008). Hydrogel nanoparticles in drug delivery. *Advanced Drug Delivery Reviews*, *60*, 1638–1649.

Hu, J., Ng, W. K., Dong, Y., Shen, S., & Tan, R. B. H. (2011). Continuous and scalable process for water-redispersible nanoformulation of poorly aqueous soluble APIs by antisolvent precipitation and spray-drying. *International Journal of Pharmaceutics*, *404*, 198–204.

Ji, J., Hao, S., Wu, D., Huang, R., & Xu, Y. (2011). Preparation, characterization and in vitro release of chitosan nanoparticles loaded with gentamicin and sylicylicacid. *Carbohydrate Polymers*, *85*, 8033–8808.

Jonassen, H., Kjøniksen, A.-L., & Hiorth, M. (2012). Effects of ionic strength on the size and compactness of chitosan nanoparticles. *Colloid and Polymer Science*, *290*, 919–929.

Katas, H., & Alpar, H. O. (2006). Development and characterization of chitosan nanoparticles for siRNA delivery. *Journal of Controlled Release*, *115*, 216–225.

Krauland, A. H., & Alonso, M. J. (2007). Chitosan/cyclodextrin nanoparticles as macromolecular drug delivery system. *International Journal of Pharmaceutics*, *340*, 134–142.

Li, P., Wang, Y., Peng, Z., She, F., & Kong, L. (2011). Development of chitosan nanoparticles as drug delivery systems for 5-fluorouracil and leucovorin blends. *Carbohydrate Polymers*, *85*, 698–704.

Lim, S., & Seib, P. A. (1993). Preparation and pasting properties of wheat and corn starch phosphates. *Cereal Chemistry*, *70*, 137–144.

Liu, Z., Jiao, Y., Wang, Y., Zhou, C., & Zhang, Z. (2008). Polysaccharides-based nanoparticles as drug delivery systems. *Advanced Drug Delivery Reviews*, *60*, 1650–1662.

Loh, J. W., Schneider, J., Carter, M., Saunders, M., & Lim, L.-Y. (2010). Spinning disc processing technology: Potential for large-scale manufacture of chitosan nanoparticles. *Journal of Pharmaceutical Science*, *99*, 4326–4336.

Makhlof, A., Tozuka, Y., & Takeuchi, H. (2011). Design and evaluation of novel pH-sensitive chitosan nanoparticles for oral insulin delivery. *European Journal of Pharmaceutical Science*, *42*, 445–451.

Nagpal, K., Singh, S. K., & Mishra, D. N. (2010). Chitosan nanoparticles: A promising system in novel drug delivery. *Chemical and Pharmaceutical Bulletin*, *58*, 1423–1430.

Nasti, A., Zaki, N. M., de Leonardis, P., Ungphaiboon, S., Sansongsak, P., Rimoli, M. G., et al. (2009). Chitosan/TPP and chitosan/TPP-hyaluronic acid nanoparticles: Systemic optimisation of the preparative process and preliminary biological evaluation. *Pharmaceutical Research*, *26*, 1918–1930.

Saboktakin, M. R., Tabatabaee, R. M., Maharramov, A., & Ramazanov, M. A. (2010). Design and characterization of chitosan nanoparticles as delivery systems for paclitaxel. *Carbohydrate Polymers*, *82*, 466–471.

Songsurang, K., Praphairaksit, N., Siraleatmukul, K., & Muangsin, N. (2011). Electrospray fabrication of doxorubicin–chitosan–tripolyphosphate nanoparticles for delivery of doxorubicin. *Archives of Pharmaceutical Research*, *34*, 583–592.

Thakur, R. K., Vial, Ch., Nigam, K. D. P., Nauman, E. B., & Djelveh, G. (2003). Static mixers in the process industries – A review. *Chemical Engineering Research and Design*, *81*, 787–826.

Xu, Y., & Du, Y. (2003). Effect of molecular structure of chitosan on protein delivery properties of chitosan nanoparticles. *International Journal of Pharmaceutics*, *250*, 215–226.

Zhang, H., Oh, M., Allen, C., & Kumacheva, E. (2004). Monodisperse chitosan nanoparticles for mucosal drug delivery. *Biomacromolecules*, *5*, 2461–2468.

Zhang, S., & Kawakami, K. (2010). One-step preparation of chitosan solid nanoparticles by electrospray deposition. *International Journal of Pharmaceutics*, *397*, 211–217.